Electrochemical Modulation of Molecular Conversion in an Azobenzene-Terminated Self-Assembled Monolayer Film: An in Situ UV−Visible and Infrared Study

ARTICLE *in* LANGMUIR · AUGUST 1997

Impact Factor: 4.46 · DOI: 10.1021/la9703555

5 AUTHORS, INCLUDING:

Rong Wang
Illinois Institute of Technology
55 PUBLICATIONS **4,462** CITATIONS

SEE PROFILE

Donald A. Tryk
University of Yamanashi
249 PUBLICATIONS **15,522** CITATIONS

SEE PROFILE

Kenkichi Hashimoto
Kyushu Medical Center
498 PUBLICATIONS **14,500** CITATIONS

SEE PROFILE

Electrochemical Modulation of Molecular Conversion in an Azobenzene-Terminated Self-Assembled Monolayer Film: An in Situ UV−Visible and Infrared Study

R. Wang,[†] T. Iyoda,[‡,§] D. A. Tryk,[†] K. Hashimoto,[†,‡] and A. Fujishima*[,†,‡]

Department of Applied Chemistry, Faculty of Engineering, The University of Tokyo, Hongo, Bunkyo-ku, Tokyo 113, Japan, and Photochemical Conversion Materials Project, Kanagawa Academy of Science and Technology Laboratory, 1583 Iiyama, Atsugi, Kanagawa 243-02, Japan

Received April 7, 1997. In Final Form: June 18, 1997[⊗]

UV−visible absorption spectroscopy and Fourier transform infrared reflection absorption spectroscopy were utilized as in situ probes to investigate the electrochemical redox process in an azobenzene-terminated self-assembled monolayer (SAM) film in an aqueous electrolyte. The electrochemical reduction process, which is exceedingly slow due to disruption of the extremely densely packed SAM, produced the hydrazobenzene species. Upon reoxidation, the resulting hydrazobenzene is quickly converted back to *trans*-azobenzene. It appears that the electrochemical redox process is accompanied by a reversible orientational change in terms of the azobenzene terminal group. Therefore, by simply modulating the applied potential, a reproducible electrochemical redox process together with a reversible orientational variation can be achieved in an organized monolayer film.

Introduction

Spontaneous organization of monolayers of molecules via adsorption on solid substrates, one form of self-assembly, is currently of considerable interest for basic research as well as for technological applications.[1] Much of this interest arises from the ease of preparation and the high degree of structural order that is present in the monolayer films. Among the various types of possible molecules and substrates, alkanethiols adsorbed onto gold surfaces have been most intensively studied. The surface of the self-assembled monolayer (SAM) can be conveniently modified by using alkanethiols terminated with various functional groups, such as carboxylic acids,[2] spiropyran,[3] ferrocene,[4] and azobenzene.[5−7] Azobenzene-based molecules are both photoactive and electrochemically active and have received a great deal of attention for their enormous potential in a variety of technological applications.[8−12] The combined photochemical and electrochemical properties of azobenzene-containing Langmuir−Blodgett (LB) films have been extensively studied by our group.[13−18] The key feature of these films is that the photochemical isomerization produces the cis form of the azobenzene moiety, which can then be selectively electrochemically reduced to hydrazobenzene. Thus, information can be stored by selectively illuminating parts of the film, with the photochemical information being latched electrochemically. This approach has also been extended to make use of selective conversion of the LB film along distinct directions using polarized UV illumination.[16] The latching process relies on the hydrazobenzene (HAB) moiety, which is both thermally stable and insensitive to the UV light that is used to stimulate the trans-to-cis photoisomerization. However, the presence of HAB is difficult to unambiguously confirm due to the requirement of spectroscopically detecting it in a monolayer in the presence of an aqueous solution. In the present work, making use of in situ Fourier transform infrared reflection absorption (FTIRRA) spectroscopic measurements,[19−26] the reversible azobenzene−hydrazobenzene redox process in an azobenzene-terminated SAM has been extensively investigated. Additionally,

* To whom correspondence should be addressed.
[†] The University of Tokyo.
[‡] Kanagawa Academy of Science and Technology Laboratory.
[§] Present address: Department of Industrial Chemistry, Faculty of Engineering, Tokyo Metropolitan University, 1−1 Minami-Ohsawa, Hachioji, Tokyo 192-03, Japan.
[⊗] Abstract published in *Advance ACS Abstracts,* August 1, 1997.

(1) Ulman, A. *An Introduction to Ultrathin Organic Films from Langmuir-Blodgett to Self-Assembly*; Academic: Boston, MA, 1991.
(2) Kim, T.; Crooks, R. M.; Tsen, M.; Sun, L. *J. Am. Chem. Soc.* **1995**, *117*, 3963.
(3) Willner, I.; Blonder, R.; Dagan, A. *J. Am. Chem. Soc.* **1994**, *116*, 9365.
(4) Rowe, G. K.; Creager, S. E. *Langmuir* **1993**, *7*, 2307.
(5) Wolf, H.; Ringsdorf, H.; Delamarche, E.; Takami, T.; Kang, H.; Michel, B.; Gerber, Ch.; Jaschke, M.; Butt, H.-J.; Bamberg, E. *J. Phys. Chem.* **1995**, *99*, 7102.
(6) Takami, T.; Delamarche, E.; Michel, B.; Gerber, Ch.; Wolf, H.; Ringsdorf, H. *Langmuir* **1995**, *11*, 3876.
(7) Caldwell, W. B.; Campbell, D. J.; Chen, K. M.; Herr, B. R.; Mirkin, C. A.; Durbin, M. K.; Dutta, P.; Huang, K. G. *J. Am. Chem. Soc.* **1995**, *117*, 6071.
(8) Wang, R.; Yang, J.; Wang, H.; Tang, D.; Jiang, L.; Li, T. *Thin Solid Films* **1995**, *256*, 205.
(9) Ichimura, K.; Momose, M.; Kudo, K.; Akiyama, H.; Ishizuki, N. *Langmuir* **1995**, *11*, 2341.
(10) Herr, B. R.; Mirkin, C. A. *J. Am. Chem. Soc.* **1994**, *116*, 1157.
(11) Caldwell, W. B.; Chen, K.; Herr, B. R.; Mirkin, C. A.; Hulteen, J. C.; Van Duyne, R. P. *Langmuir* **1994**, *10*, 4109.
(12) Campbell, D. J.; Herr, B. R.; Hulteen, J. C.; Van Duyne, R. P.; Mirkin, C. A. *J. Am. Chem. Soc.* **1996**, *118*, 10211.
(13) Liu, Z. F.; Hashimoto, K.; Fujishima, A. *Nature* **1990**, *347*, 658.
(14) Liu, Z. F.; Hashimoto, K.; Fujishima, A. *Chem. Phys. Lett.* **1992**, *185*, 501.
(15) Liu, Z. F.; Morigaki, K.; Enomoto, T.; Hashimoto, K.; Fujishima, A. *J. Phys. Chem.* **1992**, *96*, 1875.
(16) Wang, R.; Iyoda, T.; Hashimoto, K.; Fujishima, A. *J. Phys. Chem.* **1995**, *99*, 3352.
(17) Wang, R.; Iyoda, T.; Hashimoto, K.; Fujishima, A. *J. Photochem. Photobiol. A: Chem.* **1995**, *92*, 111.
(18) Wang, R.; Jiang, L.; Iyoda, T.; Tryk, D. A.; Hashimoto, K.; Fujishima, A. *Langmuir* **1996**, *12*, 2052.
(19) Laibinis, P. E.; Whitesides, G. M.; Allara, D. L.; Tao, Y. T.; Parikh, A. N.; Nuzzo, R. G. *J. Am. Chem. Soc.* **1991**, *113*, 7152.
(20) Greenler, R. G. *J. Chem. Phys.* **1966**, *44*, 310.
(21) Seki, H.; Kunimatsu, K.; Golden, W. G. *Appl. Spectrosc.* **1985**, *39*, 437.
(22) Popenoe, D. D.; Deinhammer, R. S.; Porter, M. D. *Langmuir* **1992**, *8*, 2521.
(23) Bae, I. T.; Huang, H.; Yeager, E. B.; Scherson, D. A. *Langmuir* **1991**, *7*, 1558.
(24) Nuzzo, R. G.; Fusco, F. A.; Allara, D. L. *J. Am. Chem. Soc.* **1987**, *109*, 2358.
(25) Port, S. N.; Schiffrin, D. J.; Solomon, T. *Langmuir* **1995**, *11*, 4577.
(26) Sasaki, T.; Bae, I. T.; Scherson, D. A.; Bravo, B. G.; Soriaga, M. P. *Langmuir* **1990**, *6*, 1234.

S0743-7463(97)00355-7 CCC: $14.00

evidence has been obtained for reversible changes in the orientation of the chromophore. In situ UV−visible absorption spectroscopic measurements were also used to obtain supporting information, including the kinetics of the redox processes.

Experimental Section

Chemicals. 10-(4-(Phenylazo)phenoxy)decane-1-thiol ($AzoC_{10}$) was prepared via alkylation of 4-hydroxyazobenzene with 1,10-dibromodecane and subsequent thiolation of the ω-bromide via the isothiuronium salt.[27]

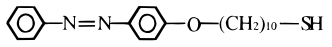

($AzoC_{10}$)

10-(4-(Phenylazo)phenoxy)decyl 1-Bromide. Ether formation was achieved by heating an ethanol solution containing 2.5×10^{-2} mol of 4-hydroxyazobenzene (Wako) and 0.11 mol of 1,10-dibromodecane (Wako) with 1.07 g of pulverized NaOH at 60 °C overnight. The resulting orange precipitate was purified by recrystallization with hexane. The isolated yield was 53%; mp 87.5−88.4 °C. Anal. Calcd for $C_{22}H_{29}BrN_2O$: C, 63.30; H, 7.00; Br, 19.15; N, 6.71; O, 3.84. Found: C, 63.64; H, 7.09; Br, 18.57; N, 6.75. ^{1}H NMR (δ, in $CDCl_3$): 1.25−1.55 (m, 12H, methylene), 1.75−1.90 (m, 4H, methylene), 3.40 (t, 2H, $-CH_2$-Br), 4.03 (t, 2H, $-OCH_2-$), 7.00 (d, 2H, phenyl ring), 7.38−7.53 (m, 3H, phenyl ring), 7.84−7.94 (m, 4H, phenyl ring). FAB mass: $[M + 1]^+ = 417.19$ and 419.19 (DMSO, magic bullet).

10-(4-(Phenylazo)phenoxy)decane-1-thiol ($AzoC_{10}$). A 7.2×10^{-3} mol amount of the bromide obtained above was dissolved in a hot mixture of 25 mL of dioxane and 6 mL of ethylene glycol containing 8.3×10^{-3} mol of thiourea (Wako). The reaction mixture was kept at 60 °C until the starting bromide was converted to the isothiuronium salt. If the bromide remained, additional amounts of thiourea were added to bring the reaction to completion. Afterward, 3 mL of tetraethylenepentamine (Wako) was added to the reaction mixture so as to decompose the isothiuronium salt to the thiol. The water-soluble nonvolatile solvent was removed by extraction, and the thiol was purified twice by recrystallization with hexane. The isolated yield was 63%; mp 82.1−83.0 °C. Anal. Calcd for $C_{22}H_{29}BrN_2O$: C, 71.31; H, 8.16; N, 7.56; O, 4.32; S, 8.65. Found: C, 71.54; H, 8.16; N, 7.71; S, 8.47. ^{1}H NMR (δ, in $CDCl_3$): 1.25−1.90 (m, 16H, methylene), 2.32 (dd, 2H, $-CH_2S-$), 4.04 (t, 2H, $-OCH_2-$), 6.97−7.03 (m, 2H, phenyl ring), 7.38−7.53 (m, 3H, phenyl ring), 7.84−7.94 (m, 4H, phenyl ring). FAB mass: $[M+1]^+ = 371.25$ (DMSO, magic bullet).

Sample Preparation. Gold films with a thickness of 15 nm were sputtered onto SnO_2-coated glass substrates (10 Ω/□, Nippon Glass Co.) for the electrochemical and in situ UV−visible spectroscopic measurements. Gold films of similar thickness were also sputtered onto the ZnSe attenuated total reflectance (ATR) element that was used to obtain the absolute FTIR spectra for $AzoC_{10}$. A high-purity gold plate mounted in Kel-F (3M) was used as a substrate for self-assembly of $AzoC_{10}$ to acquire the in situ FTIRRA spectra.

All of the gold-deposited or high-purity gold substrates were placed in contact with 1 mM $AzoC_{10}$−ethanol solution for the preparation of the SAMs. Adsorption for 2−24 h yielded reproducible monolayers. The self-assembly was accomplished in the dark to ensure that all of the azobenzene moieties were in the trans form.

Electrochemistry and UV−Visible Absorption. The electrochemical measurements were carried out in a home-built cell as reported previously.[16] In situ UV−visible absorption spectroscopic measurements were carried out using a 5 mm path length Teflon cell.[28] A reference spectrum for the $AzoC_{10}$−ethanol solution was obtained using a 1 cm path length spectrophotometric cell. The SAM-modified glass slide was attached to the electrochemical cell and served as the working electrode. A Pt wire and a saturated calomel electrode (SCE) were used as the counter electrode and reference electrodes, respectively. An initial spectrum of the SAM was collected before the electrolyte was introduced into the cell. Then, the electrolyte (0.1 M $NaClO_4$ buffered to pH 7.0 with citric acid/Na_2HPO_4 solution) was injected into the cell, with nitrogen gas purging throughout the measurements. In situ potential difference absorption spectra were recorded on a Shimadzu UV-3101PC UV−visible spectrophotometer, with the spectrum obtained at 0.0 V vs SCE being used as the reference.

Fourier Transform Infrared (FTIR) Spectroscopy. An absolute spectrum of the $AzoC_{10}$ SAM film was recorded using a ZnSe attenuated total reflection (ATR) element[29] with a sputtered layer of gold. A reference single beam spectrum R_r was collected on the gold-coated ZnSe element under N_2 prior to self-assembly. Without any mechanical movement, a 1 mM ethanol solution containing $AzoC_{10}$ was injected into the cell. After allowing 12 h for the monolayer assembly, the solution was drained and the cell was rinsed with pure ethanol to remove the residual adsorbate. After the cell was purged with nitrogen to dry the film surface, a single beam sample spectrum R_s was collected. A high signal/noise absolute spectrum was obtained in the form

$$-\Delta R/R = (R_r - R_s)/R_r \quad (1)$$

A spectroelectrochemical cell, which has previously been described by Bae et al.,[30,31] was used for the in situ FTIRRA potential difference spectroscopic measurements. The SAM was formed directly on the polished Kel-F-mounted gold electrode in the spectroelectrochemical cell in a manner similar to that for the ATR measurements. Later, the cell was filled with aqueous electrolyte (the same as that used for the in situ UV−visible spectroscopic measurements), and the gold electrode was pressed against the CaF_2 window, creating a very thin layer, typically on the order of several micrometers in thickness, in order to minimize the IR absorption of water. A Pt wire and an SCE served as the counter electrode and reference electrode, respectively. By polarization of the electrode at various potentials, potential difference FTIRRA spectra were obtained by subtraction after acquisition of single beam reflection-absorption spectra at 4 cm^{-1} resolution, using an IBM IR-98 FTIR spectrometer equipped with an MCT detector and a polarizer, which was set so as to p-polarize the incident beam. Either 500 or 2000 scans were accumulated in order to obtain acceptable signal/noise ratios.

Results and Discussion

Electrochemistry. The $AzoC_{10}$ SAM exhibited electrochemical behavior similar to that found previously for an azobenzene-containing LB film[32] in aqueous electrolyte. Figure 1 shows a set of cyclic voltammetry (CV) curves for a freshly prepared $AzoC_{10}$ SAM on a gold-coated SnO_2 glass substrate obtained with various negative switching potentials. For the most negative switching potential (−0.90 V), the cathodic current was quite large, reaching approximately 40 μA for the 1.5 cm^2 electrode (the real area was estimated to be 2.0 cm^2 on the basis of atomic force microscopic measurements). This current is largely due to hydrogen generation, which appears to be catalyzed by the SAM. The reduction process for the azo species most likely is shifted to potentials which are negative enough that the peak is obscured by the large hydrogen generation current.

When negative switching potentials below −0.95 V were used, there was evidence for film degradation, because the anodic charge (for the moment assumed to be due to HAB oxidation) decreased. Even at less negative potentials, with continuous cycling, the anodic charge gradually

(27) Cossar, B. C.; Fournier, J. O.; Fields, D. L.; Reynolds, D. D. *J. Org. Chem.* **1962**, *27*, 93.

(28) Wang, R.; Iyoda, T.; Jiang, L.; Tryk, D. A.; Hashimoto, K.; Fujishima, A. *J. Electroanal. Chem.*, in press.

(29) Bae, I. T.; Sandifer, M.; Lee, Y. W.; Tryk, D. A.; Sukenik, C. N.; Scherson, D.A. *Anal. Chem.* **1995**, *67*, 4508.

(30) Bae, I. T.; Xing, X.; Liu, C. C.; Yeager, E. *J. Electroanal. Chem.* **1990**, *284*, 335.

(31) Bae, I. T. Doctoral Dissertation, Case Western Reserve University, 1989.

(32) Liu, Z. F.; Hashimoto, K.; Fujishima, A. *J. Electroanal. Chem.* **1992**, *324*, 259.

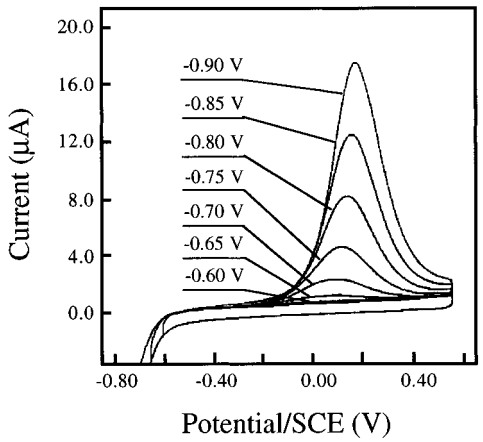

Figure 1. Cyclic voltammograms for the $AzoC_{10}$ SAM on the gold-coated SnO_2 glass substrate, taken with various negative potential limits, as labeled in each curve (electrolyte, 0.1 M $NaClO_4$ buffered to pH 7.0; potential sweep rate, 0.2 V s^{-1}; electrode area, 1.5 cm^2).

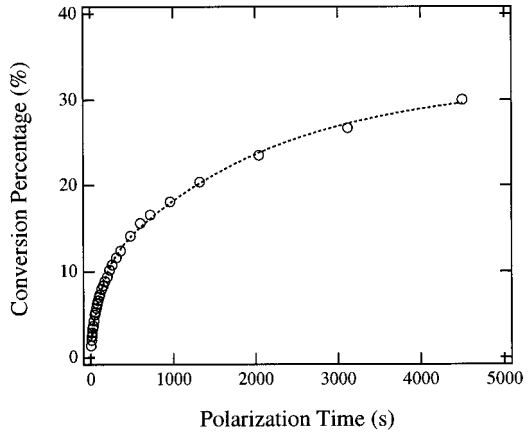

Figure 2. Percentage of conversion of the $AzoC_{10}$ SAM on gold-coated SnO_2 glass (experimental conditions as in Figure 1) to the HAB form, as a function of time, at −0.60 V vs SCE, based on the integrated anodic charge for HAB oxidation. The charge corresponding to full conversion (1.71×10^{-4} C cm^{-2}) was calculated on the basis of a molecular area of 18.7 $Å^2$.

decreased, while the characteristic redox peaks for the bare gold surface gradually grew, indicating desorption of the monolayer from the electrode. This result is consistent with results obtained by other workers for similar types of SAMs.[12] Nevertheless, the monolayers were quite stable even after more than 1 h of continuous potential cycling from −0.6 to +0.6 V at 0.2 V/s in the aqueous electrolyte. Thus, −0.6 V was chosen as a potential at which the film reduction could be examined without degradation.

The amounts of anodic charge under the oxidation peaks centered at approximately +0.20 V were used to estimate the degree of conversion from azobenzene to HAB. The calculation was based on the assumption that the resulting hydrazobenzene from the reduction of azobenzene was completely reoxidized to azobenzene. This assumption is reasonable according to the reversible CV curves as well as the reversible spectroscopic behavior, which will be discussed subsequently. The surface coverage of $AzoC_{10}$ was calculated to be 8.88×10^{-10} mol cm^{-2} based on a molecular area of 18.7 $Å^2$, which was previously obtained using high-resolution atomic force microscopy.[33] This corresponds to a theoretical charge of 1.71×10^{-4} C cm^{-2} for the two-electron process. Based on the curves in Figure 1, conversion percentages of 0.9%, 3.4%, and 7.0% were achieved for negative switching potentials of −0.7, −0.8, and −0.9 V, respectively. The conversion percentage versus polarization time at −0.6 V is plotted in Figure 2, which shows that the conversion rate is relatively slow at this potential. Although the conversion rates are faster at more negative potentials, as already stated, there is some risk of film degradation. The possible reasons for this low rate will be discussed together with the UV−visible absorption results (see below).

In Situ UV−Visible Absorption Spectroscopy. The electrochemical redox processes in the $AzoC_{10}$ SAM were monitored using in situ UV−visible absorption spectroscopy. The absorption spectrum of the as-formed $AzoC_{10}$ SAM is shown in Figure 3a (solid line). The absorption band centered at 301 nm is associated with the $\pi-\pi^*$ transition of *trans*-azobenzene, with the transition dipole moment parallel to the long axis of azobenzene.[34,35] Compared with the band position at 347 nm in dilute ethanol solution (dotted line in Figure 3a), the absorption band in the SAM exhibits a 42 nm blue shift. This shift indicates a strong H-aggregation of the azobenzene moieties in the film; i.e., they are densely packed with the long axes parallel to each other, with an orientation nearly

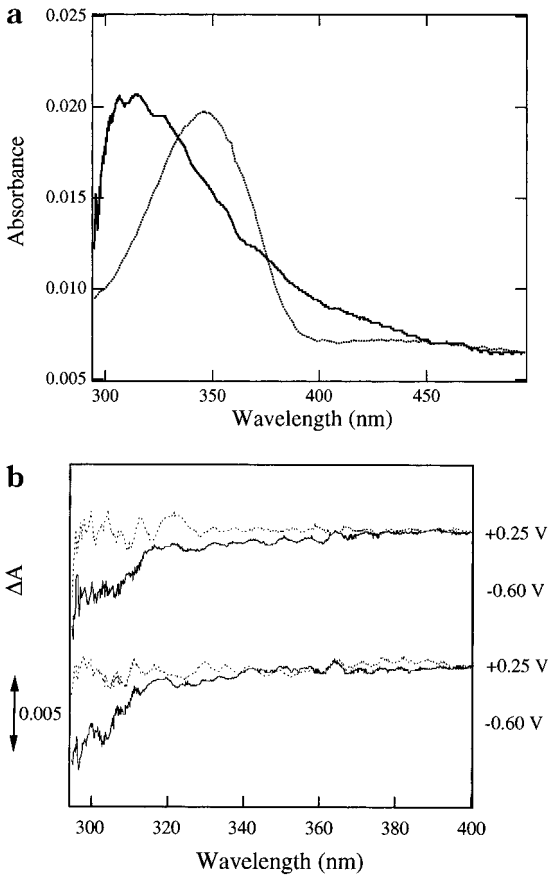

Figure 3. (a) Absolute UV−visible transmission absorption spectrum of $AzoC_{10}$ in the SAM on gold-coated SnO_2 glass (solid line) and in 3×10^{-6} M ethanol solution (dotted line). The latter, which was measured with a path length of 1.0 cm, has been multiplied by 1/4. (b) In situ difference spectra monitoring the electrochemical reduction at −0.60 V (solid line) and the following electrochemical oxidation at +0.25 V (dotted line) in the $AzoC_{10}$ SAM film. A spectrum taken at 0.0 V was used as the reference. The time required for the collection of each in situ spectrum was 20 min.

(33) Wang, R.; Iyoda, T.; Jiang, L.; Hashimoto, K.; Fujishima, A. *Chem. Lett.* **1996**, 1005.
(34) Griffiths, J. *Chem. Soc. Rev.* **1972**, *1*, 481.
(35) Kawai, T.; Umemura, J.; Takenaka, T. *Langmuir* **1989**, *5*, 1378.

perpendicular to the film surface.[33,35,36] It should be noted that, in the spectrum for the SAM shown in Figure 3a, the absorbance of the SnO_2 itself begins to become significant at close to 300 nm, so that the peak, which appears almost exactly at 300 nm when examined on a silica substrate,[28] appears to be shifted to a slightly longer wavelength. It has been shown by direct evidence, e.g., atomic force microscopy, that, for similar molecules in which azobenzene is the terminal moiety, the latter packs in ordered arrays, either "pinwheel" or herringbone-type arrays, on the SAM surface.[5,7] We have also carried out a UV−visible absorption and AFM study, in which it was shown that the structure of the $AzoC_{10}$ SAM is one in which the azobenzene moieties pack tightly in a pinwheel arrangement.[28] Our study demonstrated that, due to the very strong intermolecular interactions, the packing in this type of azobenzene-terminated SAM is significantly denser than that in the crystalline form of $AzoC_{10}$.[28] This extremely dense packing of the azobenzene moieties in the SAM is, however, inconsistent with the much looser structure proposed by Wolf et al.[5] but agrees well with the packing structure found by Caldwell et al.,[7] who confirmed this structure with extensive XRD studies.

As shown in the in situ potential difference spectra in Figure 3b, which were referenced to a spectrum obtained at 0.0 V vs SCE, the absorbance decreased significantly in the 300 nm region when the film was reduced at −0.60 V, showing that the azobenzene moieties were electrochemically bleached by the reduction procedure. The HAB species is proposed to be the reduction product due to its much lower absorption coefficient in this wavelength range.[37] This decrease in absorbance upon reduction thus provides indirect evidence of the azobenzene-to-HAB conversion. After polarization of the film at +0.25 V, the absorbance in the 300 nm range again increased, so that the difference spectrum, allowing for low-frequency oscillations, approaches a baseline, indicating the overall process to be essentially reversible. This result also suggests that the resulting HAB produced via electrochemical reduction can be completely oxidized to azobenzene. This is consistent with the CV results, even though the spectroscopic measurements were obtained using a controlled constant potential. When the potential was stepped back to −0.6 V, the absorbance in the 300 nm region again decreased, as shown in the lower set of curves in Figure 3b, showing that the behavior was reproducible.

The electrochemical redox processes were also monitored spectroscopically as a function of time. Alternate polarization of the film at −0.60 and +0.25 V gave rise to reversible absorbance changes at 305 nm, as shown in Figure 4. When the cathodic potential was set at −0.60 V, the absorbance decreased relatively slowly over a period of 20 min, approaching a constant value near the end of that period. The rate of the bleaching process was similar to that observed electrochemically, as shown in Figure 2 (discussed below).

A subsequent 20-min period of polarization at +0.25 V served to oxidize the film, and the absorbance returned to close to the initial level. The oxidation process was markedly faster than the reduction. First-order rate constants were evaluated on the basis of the data in Figure 4. It was estimated that the rate constant for reduction

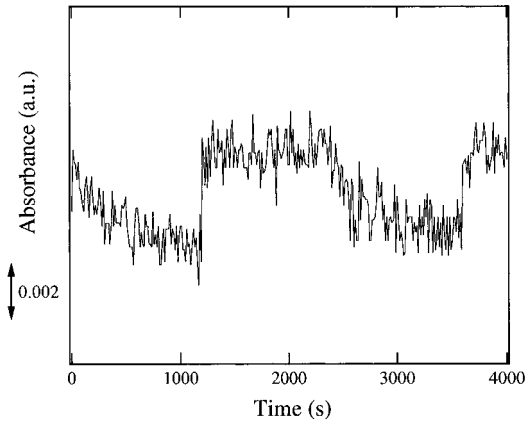

Figure 4. Changes in absorbance at 305 nm (after subtraction of the absorbance of the gold-coated SnO_2 substrate, which began to absorb strongly below 300 nm) under alternate polarization of the film between −0.60 and +0.25 V vs SCE. Each potential was held for 20 min, starting with 0.60 V.

was of the order of 10^{-5} s^{-1}, while that for oxidation was of the order of 10^{-4} s^{-1}. A probable reason for the very slow kinetics of the reduction process is that, since the interactions between neighboring azobenzene moieties are rather strong and the packing rather dense, it is quite difficult for ions to penetrate even as far as the azo nitrogens. In the study of Campbell et al., there was shown to be negligible penetration by larger ions such as tetraalkylammonium cations, while protons are able to penetrate.[12] The highly inhibited reduction process may also be explained in terms of the larger volume required by the HAB moiety, since it has been shown to have a nonplanar structure.[38] This requires a cooperative structural variation that can help relax the high steric hindrance and facilitate the reduction. As will be discussed in the following section, the cooperative variation is suggested to involve a reorientation of the terminal azobenzene moieties, which change from highly perpendicular in the azo form to inclined in the hydrazo form with respect to the film surface. The fact that the reoxidation kinetics are much faster is also an indication of the strength of the interactions between the neighboring azobenzene moieties. The strong intermolecular interaction assists the molecules to re-assemble in a highly perpendicular fashion, much as in the original self-assembly process, which has been shown to occur quite rapidly.[28] When the film was repeatedly polarized at −0.60 and +0.25 V for 20 min, the absorbance at 305 nm showed repeatable variations, indicating reproducible reduction and oxidation.

The in situ UV−visible spectroscopic study thus provides some insight into the nature of the electrochemical redox processes in the $AzoC_{10}$ SAM. Significantly, a reversible, reproducible electrochromic process was directly observed in a monolayer film.

In Situ FTIRRA Spectroscopy. The redox process in azobenzene-containing SAMs has been proposed by various workers to involve the azobenzene/HAB redox couple.[7,11,12,39,40] This was confirmed in our previous brief report via in situ FTIR investigations.[41] Campbell et al. have recently reported in situ Raman spectroscopic measurements on the electrochemical reactions of a SAM

(36) Fukuda, K.; Nakahara, H. *J. Colloid Interface. Sci.* **1984**, *98*, 555.

(37) Absorption spectra of comercially available hydrazobenzene ($C_6H_5NHNHC_6H_5$, Wako) and azobenzene ($C_6H_5N_2C_6H_5$, Wako), with the same concentration of 2.5×10^{-5} M in ethanol solution, were recorded. In the wavelength range of the $\pi-\pi^*$ transition band, the absorption coefficient for azobenzene is 18 times higher than that for hydrazobenzene.

(38) Pestena, D. C.; Power, P. P. *Inorg. Chem.* **1991**, *30*, 528.

(39) Laviron, E. *Electroanal. Chem. Interfacial Electrochem.* **1973**, *42*, 415.

(40) Blubaugh, E. A.; Yacynych, A. M.; Heineman, W. R. *Anal. Chem.* **1979**, *51*, 561.

(41) Wang, R.; Iyoda, T.; Tryk, D. A.; Hashimoto, K.; Fujishima, A.; Bae, I.; Scherson, D. A. *Chem. J. Chin. Univ.* **1995**, *16*, 125.

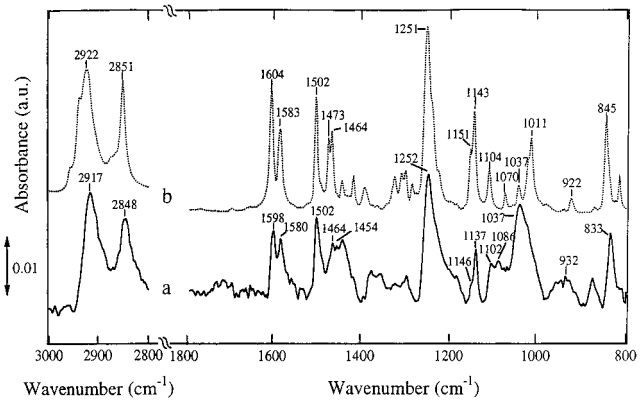

Figure 5. (a) Absolute ATR-FTIR spectrum of an $AzoC_{10}$ SAM on a gold-coated ZnSe prism using the spectrum of the substrate prior to $AzoC_{10}$ assembly as the reference. (b) Reflection absorption spectrum of $AzoC_{10}$ compound in the solid state (KBr disk).

Table 1. Peak Assignments for $AzoC_{10}$ as a Solid (KBr Disk, Figure 3, Curve b) and in the Self-Assembled Monolayer (Absolute Spectrum, Figure 3, Curve a)[a]

frequency (cm^{-1})			
KBr	SAM	vibration mode	ref
2922	2917	CH_2 asym str, d^-	19, 42, 43
2851	2848	CH_2 sym str, d^+	19, 42, 43
1604	1598	Ar str, 8a/b	44, 45, 46
1583	1580	Ar str, 8a/b	44, 45, 46
1502	1502	Ar str, 19a	44, 45, 46
1473		CH_2 scissors	19, 42, 43
1464	1464	CH_2 scissors	19, 42, 43
sh	1454	Ar str, 19b	44
1251	1252	Ph−O−R asym str	47, 48
1151	1146	Ar str, 9b	44
1143	1137	Ph−N str	18, 48
1070	1086	Ar str, 18b	44
1037	1037	Ph−O−R sym str	47, 48
1011	sh	Ar str, 18a	44
922	932	Ar str, 17b	44
845	833	Ar str, 10a	44

[a] Abbreviations: Ar = aromatic ring; asym = asymmetric; sym = symmetric; str = stretch; Ph = phenyl; R = alkyl; sh = shoulder.

composed of a ferrocenylazobenzenebutanethiol in both aqueous and nonaqueous electrolyte.[12] Their in situ Raman spectra clearly show a reversible change due to reduction of the azo group. While the new peaks are quite likely due to HAB, they were not assigned to specific vibrational modes.

In order to assign the features in the in situ measurements, an absolute spectrum of a freshly prepared $AzoC_{10}$ SAM film was collected and is shown in Figure 5 (curve a). For comparison, a spectrum of the same compound in the solid state is shown (curve b). Peak assignments and the respective peak frequencies are listed in Table 1. The bands at 2917 and 2848 cm^{-1} are assigned to the CH_2 asymmetric stretching mode ($\upsilon_{as}(CH_2)$) and symmetric stretching modes ($\upsilon_s(CH_2)$), respectively. Both of these are located at frequencies lower than those for the $AzoC_{10}$ molecules in the crystalline state (2922 and 2851 cm^{-1}, respectively). The locations of these two peaks are sensitive to the lateral interactions of the long alkyl chains. Lower frequencies indicate stronger lateral interactions and hence denser packing of the alkyl chains.[17,42,43] This suggests that the alkyl chains are densely packed in the SAM. In the lower frequency region, the 1598 and 1580

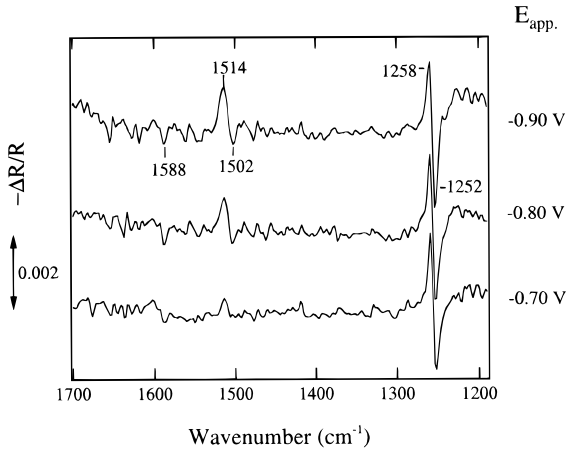

Figure 6. Series of in situ potential-difference FTIRRA spectra for an $AzoC_{10}$ SAM on a solid gold electrode. The spectrum at each potential (E_{app}) was obtained with respect to the spectrum taken at 0.0 V.

cm^{-1} bands are both assigned to the 8a/b benzene stretching modes.[44] The 1502 cm^{-1} peak is assigned to the 19a benzene stretching mode.[44] These three vibrational modes all have transition dipole moments parallel to the long axis of azobenzene.[45,46] The 1252 cm^{-1} band is assigned to the Ph−O−R (C−O−C) asymmetric stretching mode (υ_{as}(Ph−O−R)),[47,48] with the transition dipole moment perpendicular to the axis bisecting the C−O−C angle.[47] Of these, the Ph−O−R mode at 1252 cm^{-1} is the one that undergoes the most significant change as a result of the electrochemical reactions.

Figure 6 shows a series of in situ FTIRRA spectra that were obtained at three increasingly negative potentials, −0.7, −0.8, and −0.9 V, all referenced to a spectrum obtained at 0.0 V. A new positive-going peak was found at 1514 cm^{-1}, which is absent in the absolute spectrum (Figure 5). The peak intensity increased with increasingly negative applied potential. This peak is assigned to the N−H bending mode,[49−51] and the growth of the peak with negative potential is consistent with the increased fraction of molecules with the azo group in the reduced, i.e., hydrazo, form in agreement with the electrochemical and UV−visible results obtained in this study. A small negative-going peak grew in at 1588 cm^{-1} with increasingly negative applied potential, which could be associated with the 8a/b benzene stretching modes (combination of peaks at 1598 and 1580 cm^{-1}). Also, another small negative-going peak grew in at 1502 cm^{-1}, which could be tentatively assigned to the 19a benzene stretch. The intensity changes of these two bands are obscured by noise to some extent. However, these features appeared consistently in all of the potential difference spectra obtained (see Figure 7).

(42) Porter, M. D.; Bright, T. B.; Allara, D. L.; Chidsey, C. E. D. *J. Am. Chem. Soc.* **1987**, *109*, 3559.
(43) Ilharco, L. M.; Garcia, A. R.; Fidalgo, A. M.; Barros, R.; Vale, A. F.; Silva, J. L.; Silva, A. M. G. *Langmuir* **1995**, *11*, 2745.
(44) Armstrong, D. R.; Clarkson, J.; Smith, W. E. *J. Phys. Chem.* **1995**, *99*, 17825.
(45) Schoondorp, M. A.; Schouten, A. J.; Hulshof, J. B. E.; Feringa, B. L. *Langmuir* **1993**, *9*, 1323.
(46) Katayama, N.; Ozaki, Y.; Seki, T.; Tamaki, T.; Iriyama, K. *Langmuir* **1994**, *10*, 1898.
(47) Kawai, T.; Umemura, J.; Takenaka, T. *Langmuir* **1990**, *6*, 672.
(48) Nakahara, H.; Fukuda, K. *J. Colloid Interface. Sci.* **1983**, *93*, 530.
(49) A spectrum of commercially available hydrazobenzene (C_6H_5-$NHNHC_6H_5$, Wako) was recorded in a KBr disk. An intense peak at 1515 cm^{-1} was observed; however, it was absent in the spectra for $AzoC_{10}$ in both the KBr disk and the SAM film.
(50) Pretsch, E.; Clerc, T.; Seibl, J.; Simon, W. *Tabellen zur Strukturaufklärung organischer Verbindungen mit spektroskopischen Methoden*; Springer Verlag: Berlin, 1981; p 199.
(51) Lin-Vien, D.; Colthup, N. B.; Fateley, W. G.; Grasselli, J. G. *Handbook of Infrared and Raman Spectroscopy*; Academic: San Diego, CA, 1990.

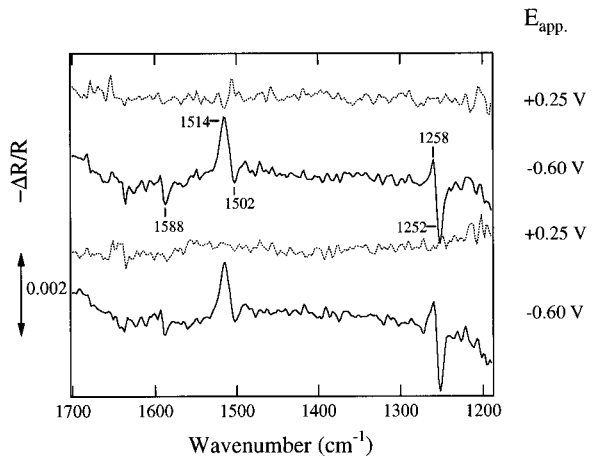

Figure 7. Series of in situ potential-difference FTIRRA spectra for an $AzoC_{10}$ SAM on a solid gold electrode obtained by switching the applied potential (E_{app}) between −0.60 and +0.25 V. The spectra were obtained with respect to the spectrum taken at 0.0 V starting with the bottom spectrum. The time required for the collection of each in situ spectrum was 20 min.

The most prominent feature of the set of spectra in Figure 6 is the unusual bipolar peak, which exhibits a positive-going spike at 1258 cm^{-1} and a negative-going spike at 1252 cm^{-1}. This feature is associated with the υ_{as}(Ph−O−R) mode. In subsequent work, it was found that the bipolar nature was associated with effects of a large increase in pH associated with H_2 evolution (water decomposition) within the thin electrolyte layer during the reduction process.[52] In that work, a similar experiment was carried out, except that it was done in such a way that there was a much smaller pH shift. In that case, there was simply a nonbipolar-type peak at 1252 cm^{-1}, which also displayed intensity changes similar to the applied potential. In any case, it is clear that the negative branch of this bipolar feature (1252 cm^{-1}) is stronger, with greater integrated intensity, than the positive branch (1258 cm^{-1}), and thus the overall effect is a loss of intensity for this vibrational mode. This aspect is also clear in the spectra shown in Figure 7. In addition, as mentioned above, when pH effects are absent, there is clearly a smaller intensity for this mode (C−O−C) when the molecules are in the reduced state.[52] Since this mode is not directly involved in the redox process, the decreased intensity may be due to a change in orientation, as discussed below.

Regarding the intensity change, we first take a general consideration. The absorption intensity is determined by Beer's law. In the present case, the absorbance $A(\upsilon)$ is described as

$$A(\upsilon) = \epsilon(\upsilon)b\Gamma f(\theta) \quad (2)$$

where $\epsilon(\upsilon)$ is the extinction coefficient at frequency υ, b is the path length of the IR probing beam through the film (constant in this case), Γ is the surface coverage of relevant molecules, and $f(\theta)$ is defined as a function of the angle θ, which is between the polarization plane of the IR probing beam and the transition moment, and $f(\theta_1) < f(\theta_2)$ when $\theta_1 > \theta_2$. $f(\theta)$ is thus regarded as a correction factor relating to the orientation of the concerned transition moment.

Considering the azobenzene−HAB molecular conversion, we define: $\Gamma_a = x\Gamma$ and $\Gamma_h = (1 - x)\Gamma$, where x and $(1 - x)$ are fractional surface coverages of azobenzene and HAB, respectively. Here the total coverage Γ is constant, and symbols with a and h subscripts correspond to the azo form and HAB form, respectively. Thereby, the absorption intensity at any frequency after electrochemical reduction can be written as

$$A(\upsilon) = A_a(\upsilon) + A_h(\upsilon) = \epsilon_a(\upsilon)xf(\theta_a)b\Gamma + \epsilon_h(\upsilon)(1 - x)f(\theta_h)b\Gamma \quad (3)$$

It should be noted that two assumptions being made here are that (1) the frequency of the particular band remains the same upon reduction and (2) the band shape also remains the same upon reduction. These assumptions are reasonable in cases in which there is no redox reaction,[19] but in the present case, where there is such a reaction, the assumptions are less certain. The fact that the vibrations in question, particularly the C−O−C stretch, do not involve the two azo nitrogens makes the assumptions reasonable, but further work is needed to thoroughly clarify this point. With respect to the absorption intensity before electrochemical reduction, i.e., $x = 1$, the difference absorption intensity $\Delta A(\upsilon)$ at a specified negative potential is

$$\Delta A(\upsilon) = A(\upsilon,x) - A(\upsilon,1) = b\Gamma(1 - x)\{\epsilon_h(\upsilon)f(\theta_h) - \epsilon_a(\upsilon)f(\theta_a)\} \quad (4)$$

From eq 4, we infer that, for a particular degree of conversion, the intensity decreases of the υ(benzene) and υ_{as}(Ph−O−R) bands could be due to either electronic changes associated with the breaking of the −N=N− double bond and the formation of the −NH−NH− bond, leading to changes in extinction coefficients, or to changes in the orientations of the corresponding transition moments. According to the standard spectra,[53] the benzene stretching bands in 1,2-diphenylhydrazine are more intense than those in azobenzene. This implies that replacing −N=N− by −NH−NH− does not reduce the extinction coefficients of the stretching bands of the adjacent benzene rings. The extinction coefficient of the υ_{as}(Ph−O−R) band is presumably also not greatly affected. This is based on the fact that the intensities for the υ_{as}-(Ph−O−R) vibrational mode for *p*-anisidine and 4-nitroanisole[51] are very similar, demonstrating that there is not a large effect of changing the nature of the group in the para position (e.g., $-NO_2$ replaced with $-NH_2$). Thus the absorbance decrease is attributed to a change in orientational correction factors, i.e., $f(\theta_h) < f(\theta_a)$, or $\theta_h > \theta_a$. Infrared surface selection rules state that the reflection−absorption measurement is sensitive to vibrational changes in the direction perpendicular to the film surface, because the electric field is polarized along the film surface normal.[20] It should be emphasized that, in the $AzoC_{10}$ molecule, all of the transition moments, which experience a decrease upon reduction, possess a similar orientation, i.e., approximately parallel to the long axis of azobenzene. The intensity decreases imply that the long axis of the azobenzene moiety inclines to a larger angle relative to the film surface normal after electrochemical reduction, and hence the perpendicular components of these transition moments decrease.

In the high-frequency region (CH_2 stretch), no variation above the noise level was detected. This observation yields the conclusion that the possible orientational changes discussed above do not involve the densely packed alkyl chains. This is reasonable, because the electrochemical reaction involves the terminal azobenzene groups, which can be accessed by solution species such as hydrated

(52) Bae, I.; Scherson, D. A.; Fujishima, A. Manuscript in preparation.

(53) *The Aldrich Library of FT-IR Spectra*, 1st ed.; Aldrich Chemical Co., Inc.: Milwaukee, WI, 1985.

protons without disturbing the strong attractive forces between the alkyl chains.[5,11,28,33]

The reproducibility of the electrochemical process was also followed using in situ FTIRRA spectroscopy. Spectra were acquired at −0.60 and +0.25 V. A total of 2000 scans were acquired for each spectrum, making the time of potential polarization (20 min) the same as that for each of the spectra presented in Figure 4. As shown in Figure 7, with a reference spectrum taken at 0.0 V, when the potential was set at −0.60 V, the spectrum is similar to those presented in Figure 6. The appearance of the 1514 cm^{-1} N−H bending mode indicates the production of HAB. The other features, including those at 1584, 1502, and 1252 cm^{-1}, are rationalized as discussed above. A noteworthy feature is that, when the potential is switched to +0.25 V, all of these characteristic features disappear, indicating that the HAB moieties, produced as a result of reduction, were completely oxidized to azobenzene and that, furthermore, the orientation of the terminal azobenzene moieties reverted back to the original one. Such cycles can be repeated several times. In addition, both the reduction process and the oxidation process did not induce any change in the high-frequency region (pertaining to the symmetric and asymmetric CH_2 stretching modes). This is due to the fact that azobenzene terminal groups assemble in a manner different from that of the alkyl chains in the $AzoC_{10}$ SAM film, according to our previous structural investigations.[28,33] The alkyl chains are not involved in the redox process. Combined with the UV−visible results shown in Figure 4, it is clear that a substantial fraction of the azobenzene moieties in the $AzoC_{10}$ SAM can be reproducibly reduced to the HAB form and then completely oxidized back to the azo form. Additionally, a reversible reorientation of the terminal functional groups occurs simultaneously.

The rate constants for the reduction and oxidation reactions have also been estimated on the basis of the time dependence of the FTIRRA spectra. Figure 8a shows a series of in situ FTIRRA spectra in the region of the N−H bending mode peak, with the film polarized at −0.60 and +0.25 V for various lengths of time. The peak intensities were integrated and plotted as a function of time in Figure 8b. Based on this, the rate constant for reduction was calculated to be on the order of 10^{-5} s^{-1}, while that for oxidation was on the order of 10^{-4} s^{-1}. These values are in agreement with those estimated on the basis of both electrochemical and UV−visible data. As has been noted previously, the different rate constants for the reduction and oxidation can be rationalized in terms of the terminal group reorientation that accompanies the electrochemical redox process.

The driving force for the orientational change is tentatively considered as follows: with the breaking of the −N=N− double bond and the formation of the −NH−NH− single bond, the terminal functional group becomes more flexible,[17] although it has been found that considerable delocalization is present in HAB, and thus the flexibility may be less than that expected for a single bond.[38] This residual stiffness, together with the nonplanar structure of the HAB molecule, implies an orientational change.

According to preliminary molecular orbital calculations, the dipole moment, which was found to be directed from the oxygen atom toward the azo group, is decreased in magnitude when the azobenzene group is replaced by a hydrazobenzene group. Considering the interaction between the molecular dipole moment and the charge of the gold electrode,[54] the dipole moment should have a tendency to align along the film surface normal when the electrode is positively charged. When the electrode is switched to a negative potential, the electronic balance may be perturbed. In addition, the azobenzene moiety is reduced to the hydrazobenzene form, which is more flexible and possesses a smaller dipole moment. Thereby, the attractive interaction between the negatively charged electrode and the relatively positively charged functional group might alter its orientation, giving rise to a larger tilt angle and setting up a new electronic balance. On the other hand, when the electrode is positively charged again, the reoxidation of the hydrazobenzene to the more rigid azobenzene helps the terminal functional groups revert back to the perpendicular orientation with respect to the film surface. The initial electronic equilibrium, which is achieved during the self-assembly process, is re-established due to the strong attractive interactions between the neighboring azobenzene moieties.

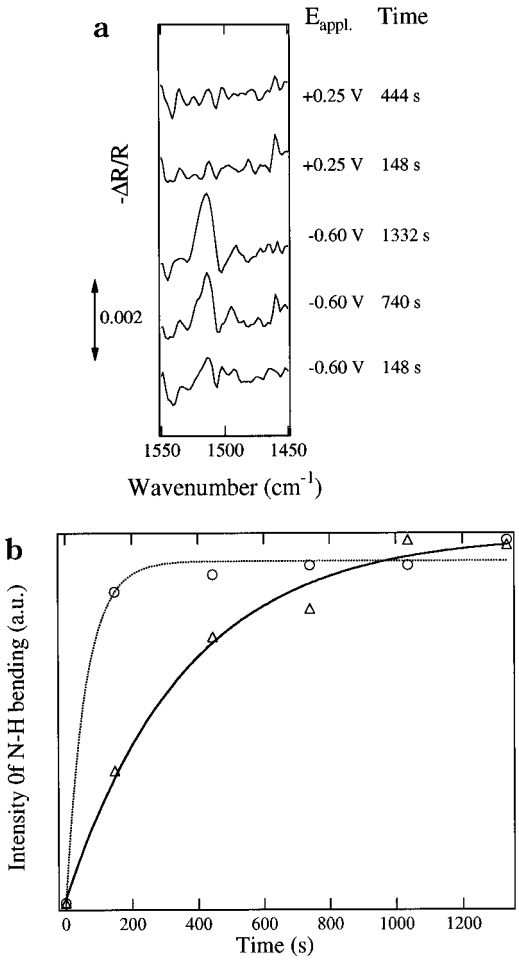

Figure 8. (a) Series of in situ potential-difference FTIRRA spectra, in the region of the N−H bending mode peak, for an $AzoC_{10}$ SAM on a solid gold electrode obtained by switching the applied potential (E_{app}) from +0.25 to −0.60 V, holding for the designated times, and then switching back to +0.25 V and holding for designated times. The spectra were obtained with respect to the spectrum taken at 0.0 V. (b) Integrated peak intensities with respect to time for the reduction process (solid line) and oxidation process (dotted line).

(54) Sato, Y.; Ye, S.; Haba, T.; Uosaki, K. *Langmuir* **1996**, *12*, 2726.

Conclusions

The electrochemical reduction and oxidation of the $AzoC_{10}$ SAM film was monitored by means of in situ UV−visible absorption and FTIRRA spectroscopies. In the in situ UV−visible spectroscopic measurements, the time dependence of the spectral changes corresponding to the reduction process was essentially the same as that obtained from the electrochemical results. The sluggishness of the reduction process is consistent with the very strong attractive interactions between the azobenzene moieties, together with the fact that HAB should have a nonplanar conformation, requiring additional space. The reproducibility of the spectral changes over several cycles is evidence for stability of the film structure. The in situ FTIRRA spectroscopic measurements furnished strong evidence, i.e., the appearance of the N−H bending mode, for the formation of the HAB moiety as the reduction product of azobenzene in the monolayer film. The bipolar nature of the C−O−C asymmetric stretching band was ascribed to the increasing pH associated with H_2 evolution in the thin electrolyte layer. The decrease in the intensity of the C−O−C asymmetric stretch and the benzene ring stretching modes indicates that the reduction of azobenzene to HAB may be accompanied by an inclination of the terminal azobenzene groups. The driving force for the reorientation is tentatively ascribed to the interaction between the charged electrode and the dipole moment of the terminal functional group. All of these changes are completely reversed upon electrochemical oxidation, which is consistent with the re-establishment of the strong intermolecular attractive forces, particularly those mediated by the azobenzene moieties. In addition, these changes appear to have virtually no effect on the orientation or packing of the alkyl chains. The present study thus provides a simple means of controlling the properties of azobenzene-based SAM films in a reversible and reproducible way.

Acknowledgment. This work was partially supported by grants from the Ministry of Education, Science, and Culture of Japan and the Japan Society for the Promotion of Science (JSPS). We thank Professor Kenjiro Hattori and Mr. Seiji Motooka, Tokyo Institute of Polytechnics, for acquiring the FAB mass data. R.W. would like to acknowledge the JSPS for financial support. The authors would like to express their great appreciation for valuable discussions and assistance with the FTIRRAS measurements, which were carried out at Case Western Reserve University with the help of Dr. In Tae Bae and Professor Daniel A. Scherson. We would also like to acknowledge helpful comments by one of the reviewers.

LA9703555